PLANAR AND COAXIAL CORE-SHELL NANOSTRUCTURES PREPARED BY ATOMIC LAYER DEPOSITION ON SEMICONDUCTOR SUBSTRATES

V. V. URSAKI[1,2], S. LEHMANN[3], V. V. ZALAMAI[1], V. MORARI[4], K. NIELSCH[3], I. M. TIGINYANU[1,2], E. V. MONAICO[1]

[1] National Center for Materials Study and Testing, Technical University of Moldova, 2004 Chisinau, Moldova
E-mail: vvursaki@gmail.com
[2] Academy of Sciences of Moldova, 2001 Chisinau, Moldova
[3] Institute for Metallic Materials (IMW), Leibniz Institute of Solid State and Materials Research (IFW Dresden), Helmholtzstr 20, 01069 Dresden, Germany
[4] Institute of Electronic Engineering and Nanotechnologies "D. Ghitu", 2028 Chisinau, Moldova

Received November 10, 2022

Abstract. Planar and core-shell structures prepared on the basis of semiconductor nanowires with various semiconductor films constitute a basis for a wide variety of devices for multiple applications. Planar structures have been prepared in this study by atomic layer deposition (ALD) of ZnO and TiO_2 thin layers on semiconductor substrates, and their morphologies and the luminescence properties have been compared with those of coaxial core-shell structures obtained by coating of GaAs nanowires with ZnO and TiO_2 shells. The prepared structures have been characterized by scanning electron microscopy (SEM), energy dispersive X-ray (EDX) and X-ray diffraction (XRD) analysis, and photoluminescence (PL) spectroscopy. Polarization characteristics of PL bands related to different recombination channels have been investigated in core-shell structures, and the results were analyzed in terms of the either contrast in dielectric constants, or selection rules associated with crystal structure symmetry, or local strain related to specific microscopic structure of recombination centers involved in electronic transitions responsible for specific PL bands.

Key words: nanowires; planar structures, coaxial core-shell structures; anodization; atomic layer deposition; scanning electron microscopy; photoluminescence spectroscopy; emission polarization.

1. INTRODUCTION

Planar structures with various semiconductor films constitute basis for a wide variety of devices. On the other hand, core-shell structures prepared on the basis of semiconductor nanowires are important building blocks for nanoelectronic and microelectronic devices, photodiodes and photovoltaics being among them. The arrays of coaxial core-shell structures demonstrate significant advantages over planar structures in such devices due to the improvement of radial charge collection, positional carrier separation and reduced reflection of the incident light,

which results in improvement of the device efficiency and cost reduction [1–4]. Quasi-one-dimensional *core-shell* structures find also applications in nonlinear optics and plasmonics [5, 6], nanophotonics [7, 8], and thermoelectrics [9].

Arrays of core-shell nanowires based on various oxide materials, such as ZnO, TiO_2, Cu_xO, $ZnFe_2O_4$, Zn_2TiO_4, GaO_xN_y are widely used in dye-sensitized solar cells and photocatalytic applications such as water splitting and pollutants removal [10–20]. Among these materials a great amount is related to those with ZnO and TiO_2 shells [11–20].

Semiconductor core-shell structures have been also explored on the basis of GaN nanowires [21–25]. Particularly, GaN–ZnO core-shell nanowires were successfully synthesized [25].

Core-shell structures with the core from narrow band gap materials have also been demonstrated in devices. Improved light absorption and efficient carrier separation has been demonstrated in n-ZnO/p-Si radial heterojunction nanowire photodiodes as compared to planar thin film diodes [1, 26, 27]. III–V materials, including GaAs, InP, and InAs have some advantages for building optoelectronic devices as compared to Si, since they are direct bandgap materials, and they have higher electron mobility [28–31].

GaAs nanowires with orientation both perpendicular and parallel to the substrate have been prepared by a cost-effective electrochemical etching, and they have been implemented in an infrared photodetector [32–34]. Core-shell structures have been prepared on the basis of these nanowires by means of electrochemical deposition of ferromagnetic metal shells [35–37].

Atomic layer deposition (ALD) is one of the most valuable techniques for growing with high accuracy conformal ultrathin films both for planar device structures and core-shell structures [38] for wide application in electrochemical energy storage, photovoltaics, photo- and electrochemical devices etc. [39].

Previous investigations showed anisotropy of the photoluminescence when recorded parallel or perpendicular to the long axis of semiconductor nanowires and core-shell structures [40–47]. Among these structures, optical properties of core-shell nanowires with GaAs core have been studied, including their polarization characteristics [34, 40, 41].

The goal of this paper is to perform a comparative study of planar and coaxial core-shell structures with ZnO and TiO_2 coatings deposited by atomic layer deposition, and to assess their optical quality be means of photoluminescence characterization.

2. MATERIALS AND METHODS

ZnO and TiO_2 shells have been deposited by atomic layer deposition on planar GaAs and GaN substrates, as well as on GaAs nanowires for the purpose of

comparison. Commercially available wurtzite n-type GaN layer (~ 2 μm thick) grown on (0001) c-plane Al_2O_3 substrates using low pressure metal organic chemical vapor deposition (MOCVD) with a free electron concentration of 2×10^{17} cm^{-3} at 295 K and threading dislocation densities of $10^9 - 10^{10}$ cm^{-2} served as GaN planar substrate, while n-type (111)B-oriented Si doped GaAs wafers, acquired from Mateck GmbH (Juelich, Germany), with a free electron concentration of 2×10^{18} cm^{-3} were used as GaAs planar substrate as well as for the preparation of GaAs nanowires arrays. GaAs nanowires were prepared by anodization of GaAs wafers cleaved into 1×1 cm^{-2} parts. The samples were subjected to several procedures before the anodization, such as sonication in acetone for 10 min, rinsing in distilled water and wet chemical etching in HCl/H_2O with a ratio of (1:3) for 2 min in order to remove the native oxide from the surface. The anodization was carried out in a cell with three electrodes configuration at applied anodic potential of 4 V. A solution of 1M HNO_3 served as electrolyte. Details of anodization have been described elsewhere [32]. Etching for 15 minutes resulted in a 45 μm thick nanostructured layer containing of GaAs nanowires oriented perpendicularly to the GaAs substrate.

ALD deposition was performed in a reactor with diethylzinc and $TiCl_4$ as Zn and Ti precursors, respectively. Deionized water (H_2O) was used as oxygen source, while high-purity N_2 served as carrier gas. The flow was kept at a rate of 20 sccm during the ALD reaction process. The optimization of the ALD-deposited ZnO thin films grown using different oxidants was recently reported [48]. The optimized $DEZ/N_2/H_2O/N_2$ pulse and purge times were 0.03/60/0.03/60 s for one ALD deposition cycle of ZnO, while these parameters for TiO_2 ($TiCl_4/N_2/H_2O/N_2$) were 0.2/120/0.015/120 s. The chamber temperature was 150°C for both ZnO and TiO_2 deposition. The growth rate of coatings was estimate to be around 0.16 nm/cycle. A number of 310 cycles was applied for ZnO and TiO_2 coatings.

The morphology and the chemical composition of samples were studied with a LEO-ZEISS Gemini 1530 scanning electron microscope (SEM) equipped with an energy dispersive X-ray (EDX) analyzer.

The photoluminescence (PL) of samples was excited by a 325 nm He-Cd laser at an excitation power density of about 1 W/cm^2, and it was analyzed with a double grating spectrometer with spectral resolution better than 1 meV. Glan–Thompson polarizers were used for polarized measurements.

3. RESULTS AND DISCUSSION

The morphology of ZnO layers deposited on planar GaN and GaAs substrates is analyzed before proceeding to investigation of their deposition on GaAs nanowires. Figure 1c illustrates that the ZnO layer deposited on a GaN substrate is quite flat and compact, and its thickness does not vary significantly on the substrate. The morphology of the layer surface deposited on a GaAs substrate (Fig. 2a and 2b)

consists basically of elongated nanoparticles with the length of (30–40) nm and the transversal dimensions around (10–15) nm, which homogeneously cover the surface, without formation of large particles. The TiO_2 coating also uniformly covers the surface of the GaAs substrate (Fig. 1d). However, the morphology is different from that of the ZnO coating, it consisting of grains with a mean size around 100 nm.

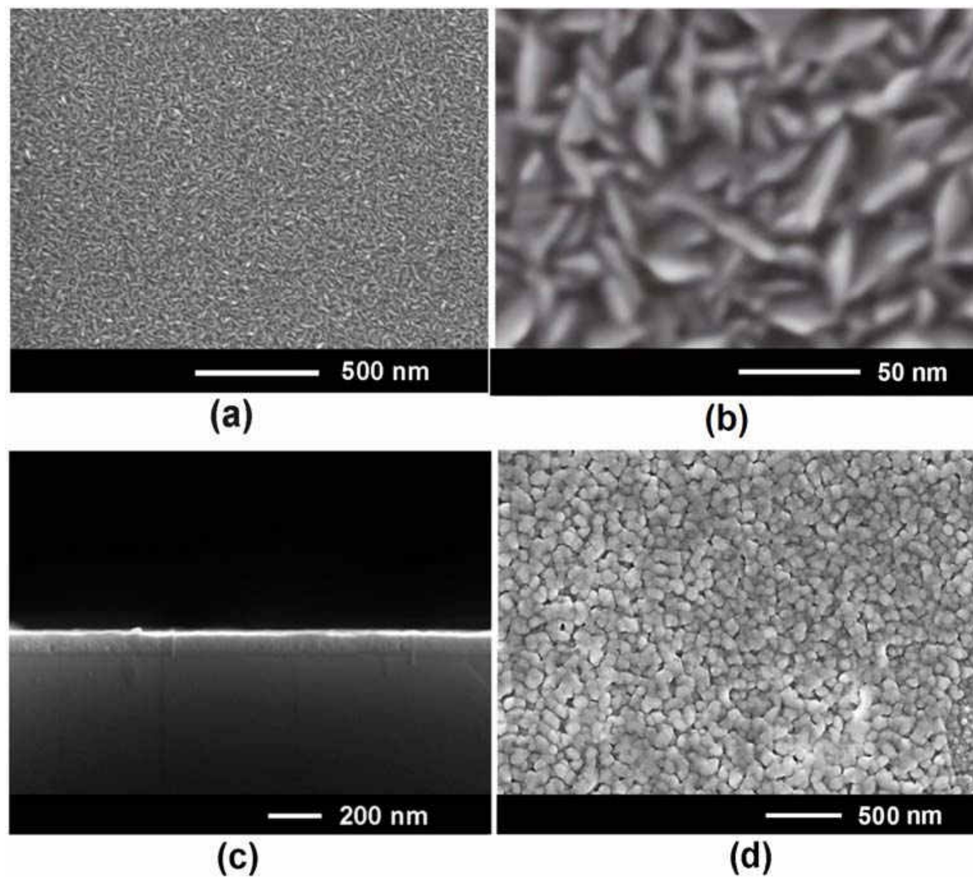

Fig. 1 – a) and b) Top view SEM images with different magnification of a ZnO layer on a GaAs substrate; c) cross section view of a ZnO layer on a GaN substrate; d) top view SEM images of a TiO_2 layer on a GaAs substrate.

The results of EDX analysis of ZnO and TiO_2 layers deposited on GaAs substrates demonstrate their nearly stoichiometric composition, within the limits of errors of the EDX system (Fig. 2), with nearly equal atomic percentage of Zn and O (Fig. 2a), and a ratio of the atomic percentage of oxygen to titanium around 2 (Fig. 2b).

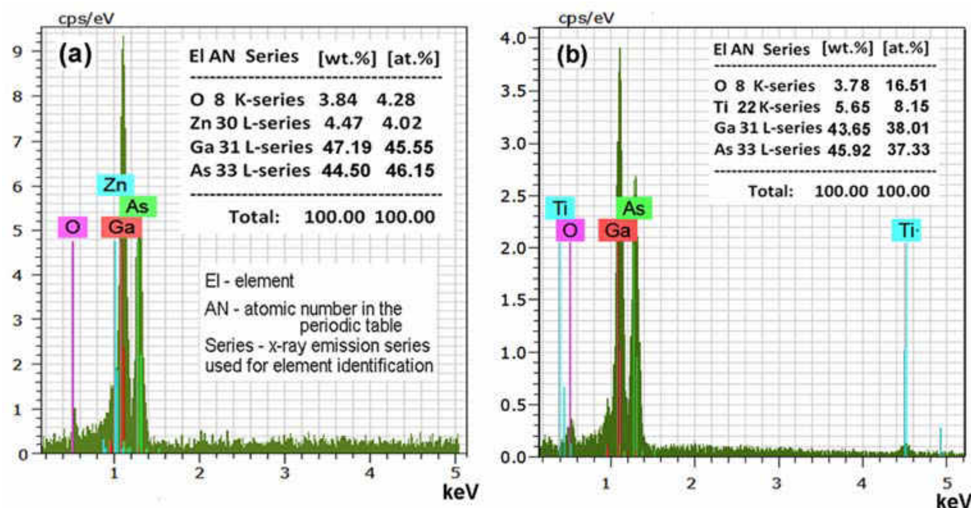

Fig. 2 – Chemical composition of thin ZnO (a), and TiO_2 (b) layers coated on GaAs substrates, as determined by EDX analysis.

The morphology of ZnO and TiO_2 coating on GaAs wires is in some extent different from that of a ZnO layer deposited on a flat GaAs substrate (Fig. 3). The GaAs nanowires prepared by anodization of (111)B substrates in 1M HNO_3 electrolyte for 15 minutes are of a length of 45 μm, and they are oriented predominantly perpendicularly to the substrate surface (Fig. 3a) [35]. The thickness of coatings on GaAs nanowires is estimated to be around 50 nm, and their morphology consists of grains with mean size around 50 nm for both the ZnO and TiO_2 coatings. However, the grain sizes are more uniform for the TiO_2 coating as compared to the ZnO layer. This observation is also valid for coatings on planar GaAs substrates, as illustrated in Figs. 1b and 1d. At the same time, the dimensions of grains are different for coatings on planar substrates and those on nanowires, which suggest that the ALD process is influenced by the state of the GaAs surface, the roughness of GaAs nanowires being influenced by some current oscillations occurring during the anodization process.

Similarly to coatings on planar substrates, the chemical composition of layers on GaAs nanowires is nearly stoichiometric, the atomic percentage of Zn and O being nearly equal within the limits of errors of the EDX system (Fig. 3c), and the ratio of the atomic percentage of oxygen to titanium being around 2 (Fig. 3d).

Further analysis is focused on the photoluminescence of ZnO layers deposited on GaN substrates. The luminescence spectrum from a ZnO layer on a GaN substrate is shown in Fig. 4. The luminescence measured at low temperature (Fig. 4a) comes mainly from the GaN substrate, and it is dominated by the excitonic emission at 3.481 eV related basically to the recombination of excitons bound to neutral donors

(D^0X) [49]. A weaker PL band is also observed in the region of (3.40–3.42) eV, which was previously associated with electron transitions from a donor-type energy band to a defect-related acceptor level in GaN [50]. A series of weak lower energy bands at 3.306 eV, 3.068 eV, 2.993 eV, 2.900 eV, 2.815 eV, and 2.704 eV can be attributed to deeper, unidentified, point defects and complexes in the GaN substrate. Since the intensity of the emission from the GaN substrate at low temperature is much higher than that from the ZnO coating, no PL bands related to the ZnO layer are observed in the spectrum. On the other hand, with increasing the temperature, the emission from the GaN substrate is quenched faster, as compared to that coming from the ZnO coating. As a result, a PL band at 3.36 eV related to near-band-gap recombination in the ZnO layer emerges in the spectrum measured at room temperature (curve 2 in Fig. 4b).

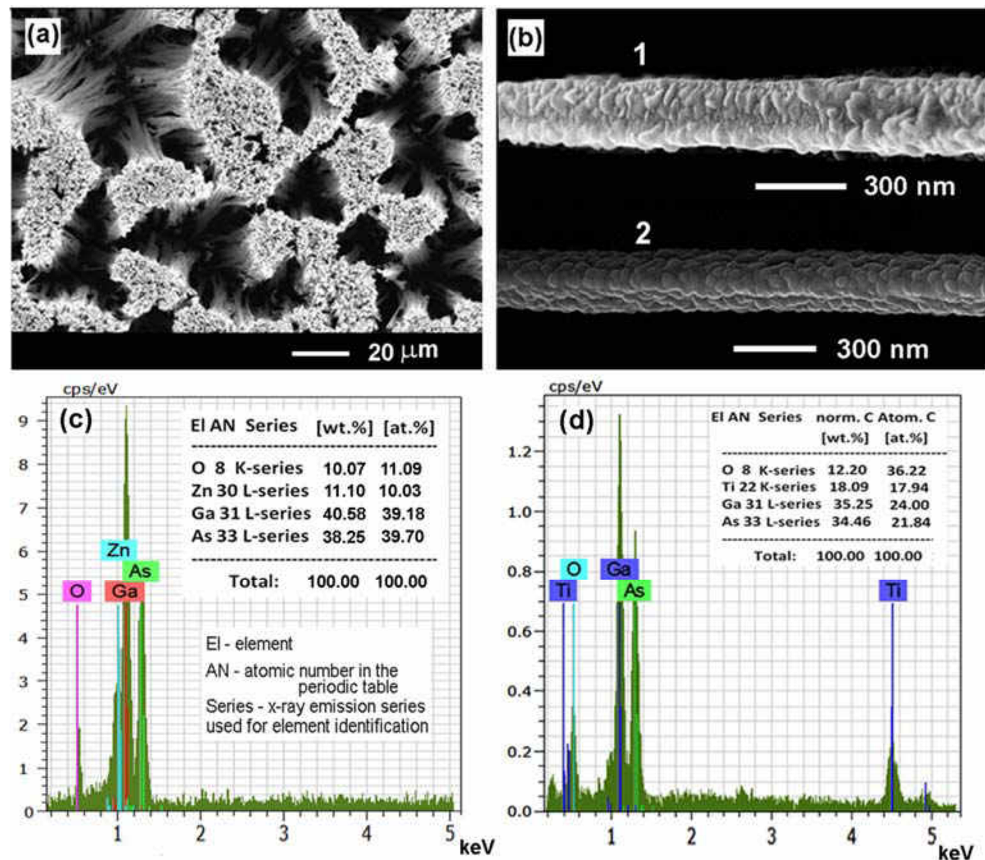

Fig. 3 – a) Top view SEM images of a GaAs nanowire array produced by anodizing a GaAs substrate with (111)B crystallographic orientations; b) SEM image of a single GaAs nanowire with a ZnO shell (1), and a GaAs nanowire with a TiO_2 shell (2); c) chemical composition of the ZnO layer on the GaAs nanowires; d) the same for the TiO_2 layer.

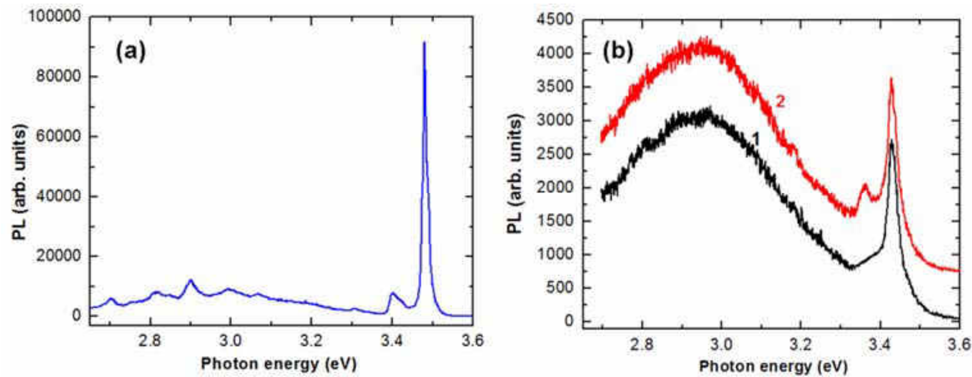

Fig. 4 – a) PL spectrum of a GaN sample coated with a ZnO layer measured at 10 K; b) PL spectra of a GaN sample (curve 1), and a GaN sample coated with a ZnO layer (curve 2) measured at 300 K.

This analysis shows that luminescence from the GaN substrate is much more intensive than that from the ZnO coating, which makes this material system not too relevant for exploring the polarization effects in luminescence from structures with a GaN core and ZnO shell. Therefore, the further investigation will be focused on coaxial structures with a GaAs core and a ZnO shell.

The luminescence of GaAs/ZnO core-shell structures consists of emission in two spectral range, namely the emission in the infrared (IR) region (Fig. 5a, left column) coming from the GaAs core, and the emission in the ultraviolet (UV) region (Fig. 5b, right column) coming from the ZnO shell.

The spectrum from the GaAs core is composed of three PL bands at 1.486 eV, 1.360 eV and 1.310 eV. The nature of the emission band at 1.486 eV has been investigated in previous works [51–55], and it was assigned to donor-acceptor pair (DAP) recombination, or to free-to-bound transition with the participation of a Si_{As} acceptor. Three recombination channels have been proposed to explain the nature of the PL band at 1.360 eV [52–54], namely electron transitions to gallium-vacancy complex, or to arsenic-vacancy complex, or to Cu_{Ga} centers.

The spectrum from the ZnO shell consists of a high energy PL band at 3.360 eV band and a series of lower energy bands. The high energy PL band at 3.360 eV is usually observed in high-quality ZnO crystals [56–59], and it is suggested to be related to recombination of excitons bound to neutral donor impurities (D^0X). The donor in the case of GaAs/ZnO core-shell structures is most probably associated with Ga atoms incorporated into the ZnO shell due to diffusion of the Ga impurity from the GaAs core during the ALD process. The band at 3.328 eV was previously assigned to emission of excitons bound to structural defects [56], while the band at 3.310 eV was associated with DAP recombination [58, 59].

The analysis of Fig. 5 shows that the polarization of excitonic emission from the ZnO shell depends on the nature of defects to which the excitons are bound.

The PL emission from excitons bound to neutral donors is polarized preponderantly in the radial direction of core-shell structure, while the emission from excitons bound to structural defects is polarized preponderantly along the nanowires. The other lower energy PL bands are also polarized preponderantly along the nanowires. The same trends are characteristic for the emission from the GaAs core, *i.e.* the emission with high photon energy is polarized preponderantly in the radial direction of core-shell structure, while the emission with low photon energy is polarized preponderantly along the nanowires. That means that the emission related to shallow/deep recombination centers is polarized in the radial/axial direction of nanowires.

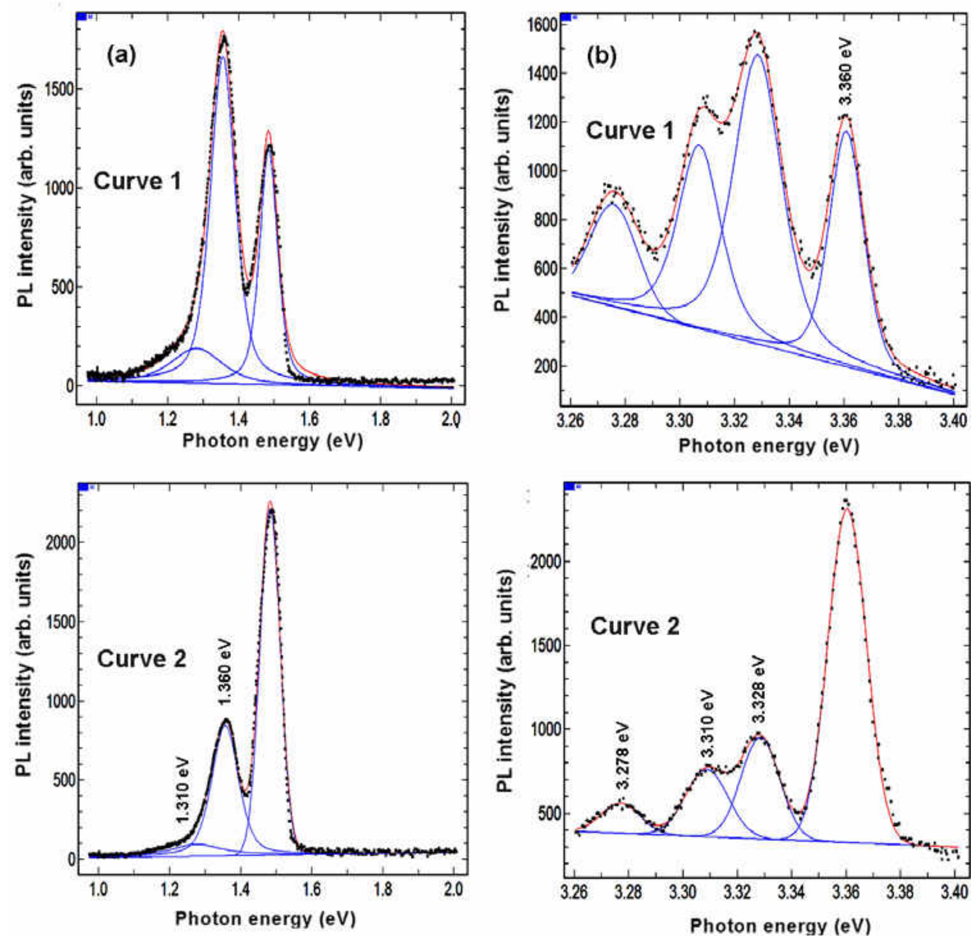

Fig. 5 – PL spectra of the GaAs core (a, left column) and ZnO shell (b, right column) measured at 10 K with the emission polarized along the nanowire axis (curve 1), and polarized in the radial direction (curve 2).

According to the classical electromagnetic theory, the polarization of the emission along the axes of semiconductor nanowires is due to the large contrast in dielectric constants of the semiconductor nanowires and their environments [40, 43]. On the other hand, the emission polarization may be determined by the symmetry of the crystal structure, it being polarized along the nanowire axis in materials with zincblende (ZB), or perpendicularly to the nanowire axis in materials with wurtzite (WZ) structure [41, 42]. It was also previously found that strains may strongly influence on the emission polarization, especially on emission related to defects or clusters. So, that the emission associated with excitons bound at defect clusters in nanowires with ZB structure is polarized in the direction perpendicular to the nanowire axis instead of polarization along the nanowire axis [45, 46]. The effect was explained in terms of tensile local strain experienced by defect clusters. The change of the polarization direction of the emission due to strain was also observed in nanowires with WZ structure [47].

Concerning the materials presented in this paper, one should note that the GaAs core of nanowires has ZB structure, while the ZnO shell is of WZ structure. So that the predominant polarization of the excitonic D^0X band in the WZ ZnO shell perpendicularly to the nanowire axis is due to the crystal structure symmetry with a negligible effect from the contrast in dielectric constants. On the other side, the predominant polarization of the lower energy PL bands along the nanowire axis is either due to the contrast in dielectric constants, or to local strain related to impurities or defects responsible for these PL bands.

The predominant polarization of the PL band at 1.486 eV in the GaAs core perpendicularly to the nanowire axis, instead of polarization along the nanowires axis expected both from the point of view of the contrast in dielectric constants and from the crystal structure symmetry, may come from the specific microscopic structure of the defects responsible for this PL band and from strain they experience. The polarization of the lower energy PL band at 1.360 eV along the nanowire axis is due to the contrast in dielectric constants.

4. CONCLUSIONS

ZnO and TiO_2 coatings have been deposited by atomic layer deposition on planar GaAs and GaN substrates as well as on GaAs nanowires produced by anodization of (111)B GaAs wafers for the purpose of comparison. The arrays of GaAs nanowires were found to be oriented predominantly perpendicularly to the substrate surface, which made it possible to investigate the polarization characteristics of luminescence from the prepared coaxial core-shell structures. The EDX analysis demonstrated nearly stoichiometric composition of ZnO and TiO_2 coatings both on GaAs nanowires and on planar substrates. The morphology of ZnO and TiO_2 coatings on GaAs wires was found to be different from that of layers deposited on

a flat GaAs substrate in terms of dimensions and forms of grains. The difference was explained by different state of the GaAs surface on the flat substrate and on nanowires, the roughness of GaAs nanowires being influenced by some current oscillations occurring during the anodization process.

The performed analysis showed that the luminescence from the ZnO coating is significantly weaker than the emission from the GaN substrate, which makes this material system less relevant for exploring the polarization effects in luminescence as compared to coaxial GaAs-ZnO core-shell structures. The predominant polarization of the D^0X emission from the ZnO shell perpendicularly to the nanowire axis was explained by selection rules associated with crystal structure symmetry. The predominant polarization of the emission associated with shallow impurities in the GaAs core in the radial direction of core-shell structure was suggested to be associated with local strain around these shallow recombination centers. The predominant polarization of the emission related to deeper recombination centers from both the GaAs core and ZnO shell along the nanowires axis was explained in terms of the contrast in dielectric constants of the components of the core-shell structures and the environments.

Acknowledgements. This research was funded by National Agency for Research and Development of Moldova under the Grants #21.00208.5007.15/PD and #20.80009.5007.20, and by European Commission under the H2020 grant #810652 'NanoMedTwin'. V.M. acknowledges support from the German Academic Exchange Service for DAAD scholarship at IFW Dresden (Germany).

REFERENCES

1. K. Y. Ko, H. Kang, J. Kim, W. Lee, H. S. Lee, S. Im, J. Y. Kang, J.-M Myoung, H.-G. Kim, S.-H. Kim *et al.*, Mater. Sci. Semicond. Proces. **27**, 297–302 (2014).
2. A. Nduwimana, R. N. Musin, M. Smith, X.-Q. Wang, Nano Lett. **8**, 3341–3344 (2008).
3. Y. Zhang, L.-W. Wang, A. Mascarenhas, Nano Lett. **2007**(7), 1264–1269, doi:10.1021/nl070174f.
4. K.-Y. Pan, Y.-H. Lin, P.-S. Lee, J.-M. Wu, H. C. Shi, J. Nanomater. **2012**(2012), 1–6, doi:10.1155/2012/279245.
5. S. Ramadurgam, T.-G. Lin, C. Yang, J. Mater. Sci. Technol. **31**, 533–541 (2015).
6. R. Grange, *Nonlinear Optical Enhancement with Plasmonic Core-Shell Nanowires*, in L. De Sio (Eds.), *Active Plasmonic Nanomaterials*, Pan Stanford Publishing Pte. Ltd, New York, 2015; Chapter 10, pp. 323–342.
7. M. S. Gudiksen, L. J. Lauhon, J. Wang, D. C. Smith, C. M. Lieber, Nature **415**, 617–620 (2002).
8. D. Shao, H. Sun, G. Xin, J. Lian, S. Sawyer, S. Appl. Surf. Sci. **314**, 872–876 (2014).
9. R. Mulla, C. W. Dunnill, Mater. Adv. **3**, 125–141 (2022).
10. C. Florica, A. Costas, N. Preda, M. Beregoi, A. Kuncser, N. Apostol, C. Popa, G. Socol, V. Diculescu, I. Enculescu, Sci. Rep. **9**, 17268 (2019).
11. H.-J. Son, C. H. Kim, D. W. Kim, N. C. Jeong, C. Prasittichai, L. Luo, J. Wu, O. K. Farha, M. R. Wasielewski, J. T. Hupp, ACS Appl. Mater. Interfaces **7**, 5150–5159 (2015).
12. M. Law, L. E. Greene, A. Radenovic, T. Kuykendall, J. Liphardt, P. Yang, J. Phys. Chem. B **110**, 22652–22663 (2006).
13. L.-C. Chen, S.-F. Tsai, J.-H. Chen, G.W. Wang, Int. J. Photoenergy **2013**, 1–9 (2013).
14. Y. Zhao, P. Tong, D. Ma, B. Li, Q. Liu, S. Chen, Y. Zhang, J. Chemistry **2017**, 1–8 (2017).

15. M. Liu, C.-Y. Nam, C. T. Black, J. Kamcev, L. Zhang, J. Phys. Chem. C **117**, 13396–13402 (2013).
16. L. Liu, H. Wang, D. Wang, Y. Li, X. He, H. Zhang, J. Shen, Crystals **10**, 325 (2020).
17. J. Park, P. R. Deshmukh, Y. Sohn, W. G. Shin, J. Alloys Comp. **787**, 1310–1319 (2019).
18. J.-J.Tao, H.-P. Ma, K.-P Yuan, Y. Gu, J.-W. Lian, X.-X. Li, W. Huang, M. Nolan, H.-L. Lu, D.-W. Zhang, Nanoscale **12**, 7159–7173 (2020).
19. L. Movsesyan, A. Maijenburg, N. Goethals, W. Sigle, A. Spende, F. Yang, B. Kaiser, W. Jaegermann, S.-Y. Park, G. Mul, C. Trautmann, M. E. Toimil-Molares, Nanomaterials **8**, 693 (2018).
20. K. Jeong, P. R. Deshmukh, J. Park, Y. Sohn, W. G. Shin, *ACS Sustainable*, Chem. Eng. **6**, 6518–6526 (2018).
21. P. Ruterana, M. Albrecht, J. Neugebauer (Eds.), Nitride Semiconductors: *Handbook on Materials and Devices*, Berlin, Wiley-VCH, 2003.
22. Y. Kang, X. Liu, D. Wang, S. Fang, Y. Luo, H. Sun, JUSTC **52**, 2 (2022).
23. Q. C. Bui, L. Largeau, M. Morassi, N. Jegenyes, O. Mauguin, L. Travers, X. Lafosse, C. Dupuis, J.-C Harmand, M. Tchernycheva, N. Gogneau, App. Sci. **9**, 3528 (2019).
24. L. Lari, I. M. Ross, T. Walther, K. Black, C. Cheze, L. Geelhaar, H. Riechert, P. R. Chalker, J. Phys.: Conf. Ser. **471**, 012039 (2013).
25. H. W. Kim, J. C. Yang, H. G. Na, C. Le, Appl. Surf. Sci. **257**, 9420–9424 (2011).
26. H.-D. Um, S. A. Moiz, K.-T. Park, J.-Y. Jung, S.-W. Jee, SC. H. Ahn, D. C. Kim, H. K. Cho, D.-W. Kim, J.-H. Lee, Appl. Phys. Lett. **98**, 033102 (2011).
27. H. Kang, J. Park, T. Choi, H. Jung, K. H. Lee, S. Im, H. Kim. Appl. Phys. Lett. **100**, 041117 (2012).
28. X. Shen, M. Yao, K. Sun, T. Zhao, Y. He, C.-Y. Chi, C. Zhou, P. D. Dapkus, N. S. Lewis, S. Hu, ACS Energy Lett. **6**, 193–200 (2021).
29. M. Royo, M. De Luca, R. Rurali, I. Zardo. J. Phys. D: Appl. Phys. **50**, 143001 (2017).
30. X. Gao, D. Fang, X. Fang, J. Tang, F. Fang, J. Li, X. Chu, X. Wang, Z. Wei. Mater. Res. Express **2**, 095902 (2105).
31. J. A. Czaban, D. A. Thompson, R. R. LaPierre. Nano Lett. **9**, 148–154 (2009).
32. E. Monaico, I. Tiginyanu, V. Ursaki. Semicond. Sci. Technol. **35**, 103001 (2020).
33. E. I. Monaico, E. V. Monaico, V. V. Ursaki, S. Honnali, V. Postolache, K. Leistner, K Nielsch, I. M. Tiginyanu, Beilstein J. Nanotechnol. **11**, 966–975 (2020).
34. V. V. Ursaki, S. Lehmann, V. V. Zalamai, V. Morari, K. Nielsch, I. M. Tiginyanu, E. V. Monaico, Crystals **2022**(12), 1145 (2022).
35. V. Monaico, V. Morari, V. V. Ursaki, K. Nielsch, I. M. Tiginyanu, Nanomaterials **12**, 1506 (2022).
36. E. V. Monaico, V. Morari, M. Kutuzau, V. V. Ursaki, K. Nielsch, I. M. Tiginyanu, Materials **15**, 6262 (2022).
37. E. V. Monaico, V. Morari, M. Kutuzau, V. V. Ursaki, K. Nielsch, I. M. Tiginyanu, Rom. J. Phys. **67**, 611 (2022).
38. A. J. Austin, E. Echeverria, P. Wagle, P. Mainali, D. Meyers, A. K. Gupta, R. Sachan, S. Prassana, D. N. McIlroy, Nanomaterials **10**, 2434 (2020).
39. J. Bachmann, (Ed.), *Atomic Layer Deposition in Energy Conversion Applications*, Wiley-VCH Verlag GmbH & Co KGaA, Weinheim, Germany, 2017.
40. T. B. Hoang, L. V. Titova, H. E. Jackson, L. M. Smith, J. M. Yarrison-Rice, Y. Kim, H. J. Joyce, C. Jagadish, Proceedings of the 2006 Sixth IEEE Conference on Nanotechnology, Cincinati, OH, USA, 17–20 July 2006; Volume 1, pp. 116–118.
41. B. V. Novikov, S. Yu Serov, N. G. Filosofov, L. V. Shtrom, V. G. Talalaev, O. F. Vyvenko, E. V. Ubyivovk, Yu. B. Samsonenko, A. D. Bouravleuv, I. P. Soshnikov, N. V. Sibirev, G. E. Cirlin, V. G. Dubrovskii, Phys. Status Solidi RRL **4**, 175–177 (2010).
42. A. Mishra, L. V. Titova, T. B. Hoang, H. E. Jackson, L. M. Smith, J. M. Yarrison-Rice, Y. Kim, H. J. Joyce, Q. Gao, H. H. Tan, C. Jagadish, Appl. Phys. Lett. **91**, 263104 (2007).
43. C. X. Shan, Z. Liu, S. K. Hark, Phys. Rev. B **74**, 153402 (2006).

44. G. Jacopin, L. Rigutti, A. D. Bugallo, F. H. Julien, C. Baratto, E. Comini, M. Ferroni, M. Tchernycheva, Nanoscale Research Lett. **6**, 501 (2011)
45. S. Filippov, S. Sukrittanon, Y. Kuang, C. Tu, P. O. A. Persson, W. M Cen, I. A. Buyanova, Nano Lett. **9**, 5264–5269 (2014).
46. I. A. Buyanova, W. M. Chen, Nanotechnology **30**, 292002 (2019).
47. G. Jacopin, L. Rigutti, S. Bellei, P. Lavenus, F. H. Julien, A. V. Davydov, D. Tsvetkov, K. A. Bertness, N. A. Sanford, J. B. Schlager, M. Tchernycheva, Nanotechnology **23**, 325701 (2012).
48. J. Yang, A. Bahrami, X. Ding, S. Lehmann, N. Kruse, S. He, B. Wang, M. Hantusch, K. Nielsch, Adv. Materials Inter. **9**, 2101953 (2022).
49. V. V. Ursaki, I. M. Tiginyanu, V. V. Zalamai, S. M. Hubbard, D. Pavlidis, J. Appl. Phys. **94**, 4813 (2003).
50. V. V. Ursaki, I. M. Tiginyanu, V. V. Zalamai, V. M. Masalov, E. N. Samarov, G. A. Emelchenko, F. Briones, Semicond. Sci. Technol. **19**, 851–854 (2004).
51. K. Kudo, Y. Makita, I. Takayasu, T. Nomura, T. Kobayashi, T. Izumi, T. Matsumori, J. Appl. Phys. **59**, 888–891 (1986).
52. E. W. Williams, H. Barry Bebb. *Photoluminescence II: Gallium Arsenide*, in: R. K. Willardson, A. C. Beer (Eds.), Vol. 8, Academic Press, New York and London, 1972, Chapter 5, pp. 321–392.
53. V. Swaminathan, R. Caruso, S. J. Pearton, J. Appl. Phys. **63**, 2164–2167 (1988).
54. K. C. Shin, M. H. Kwark, M. H. Choi, M. H. Oh, Y. B. Tak, J. Appl. Phys. **65**, 736–741 (1989).
55. T. Itoh, M. Takeuchi, Jpn. J. Appl. Phys. **16**, 227–232 (1977).
56. B. K. Meyer, H. Alves, D. M. Hofmann, W. Kriegseis, D. Forster, F. Bertram, J. Christen, A. Hoffmann, M. Straßburg, M. Dworzak, U. Haboeck, A. V. Rodina, *Bound Exciton and Donor–Acceptor Pair Recombinations in ZnO*, Phys. Stat. Sol. (b) **2004**(241), 231–260, doi:10.1002/pssb.200301962.
57. V. V. Ursaki, I. M. Tiginyanu, V. V. Zalamai, E. V. Rusu, G. A. Emelchenko, V. M. Masalov, E. N. Samarov, Phys. Rev. B **70**, 155204 (2004).
58. V. V. Ursaki, I. M. Tiginyanu, V. V. Zalamai, V. M. Masalov, E. N. Samarov, G. A. Emelchenko, F Briones, J. Appl. Phys. **96**, 1001–1006 (2004).
59. V. V. Ursaki, I. M. Tiginyanu, V. V. Zalamai, V. M. Masalov, E. N. Samarov, G. A. Emelchenko, F. Briones, Semicond. Sci. Technol. **19**, 851–854 (2004).